Published in "Photochemical & Photobiological Sciences 6: 956-963, 2007"
which should be cited to refer to this work.

Ultrafast excited-state dynamics of phenyleneethynylene oligomers in solution

Guillaume Duvanel[a], **Jakob Grilj**[a], **Anne Schuwey**[b], **Albert Gossauer**[b] **and Eric Vauthey***[a]

[a] *Department of Physical Chemistry of the University of Geneva, 30 quai Ernest-Ansermet, CH-1211, Geneva 4, Switzerland. E-mail: eric.vauthey@chiphy.unige.ch*

[b] *Department of Chemistry of the University of Fribourg, Pérolles, CH-1700, Fribourg, Switzerland*

The excited-state dynamics of oligomeric phenyleneethynylenes (OPEs) of various length and substitution has been investigated by femtosecond time-resolved spectroscopy. The fluorescence lifetime of the OPEs decreases with the number of phenyleneethynylene units up to about 9. This effect is due to an increase of the oscillator strength for the S_1–S_0 transition. Dynamic features occurring within a few tens of picoseconds and ascribed to structural relaxation directly after population of the S_1 state can be observed in non-viscous solvents. The effect of torsional disorder on the fluorescence intensity is shown to depend strongly on the nature of the substituent on the phenyl groups. All these effects are qualitatively discussed with a simple exciton model.

Introduction

Over the past decade, conjugated polymers have attracted a considerable attention because of their electronic properties, which open promising perspectives of applications in various areas of electronics and photonics.[1–3] Among these polymers, poly(*p*-phenyleneethynylene)s (PPEs)

are characterized by a highly conjugated, rigid and linear structure, which makes them particularly well suited to be used as 'molecular wires'.[4–6] For these reasons, oligomeric *p*-phenyleneethynylenes (OPEs) are often used as building blocks in complex nanometer-scale molecular architectures.[7–9] PPEs and OPEs exhibit intense absorption in the UV-visible at a wavelength increasing with the number of phenyleneethynylene (PE) units, *N*.[10] This property has been used advantageously in the development of light-harvesting antennae based on PE dendrimers.[11,12] PPEs are also highly emissive and thus have been shown to be a possible alternative to poly(*p*-phenylenevinylene)s in electroluminescent devices.[5]

The optical spectra of OPEs are characterized by a substantial asymmetry between absorption and fluorescence. Indeed, the absorption band associated with the S_0–S_1 transition is broad and structureless, while the corresponding fluorescence band is narrower and structured. Moreover, the Stokes shift between both bands is very small. These effects have been explained in terms of torsional disorder and quadratic coupling between the ground and the first singlet excited states.[13] The twisting about the long molecular axis of OPEs is relatively free in the ground state, while it is much more constrained to a planar geometry in the excited state due to the effect of quinoidal/cumulenic configurations. As a consequence, the ground- and excited-state potentials have very different curvature along the torsional coordinate. This quadratic coupling model predicts a narrowing of the blue edge fluorescence spectrum as a function of time, which has been confirmed experimentally for an OPE with $N = 9$.[13]

Recent time-resolved resonance Raman measurements on 1,4-bis(phenylethynyl)benzene have shown that this molecule in the S_1 state has not a strong quinoidal/cumulenic structure but is still characterised by an acetylenic character.[14] Moreover, a 50 ps rise of the Raman signal, assigned to structural changes, was observed.

More recently, the shift to longer wavelength and the broadening of the absorption band with increasing number of PE units have been reproduced using an exciton model for the excitation energy.[15] Other quantum chemical calculations of PPEs and OPEs have also been reported in literature.[16–18] However, there has been, to our knowledge, no systematic study of the effect of length and substitution on the excited-state dynamics of OPEs.

We report here on our investigation of the excited-state dynamics of several OPEs, which, as shown in Fig. 1, differ by the number of PE units, $N = n + 1$, and by their substituents, using femtosecond-resolved absorption and fluorescence spectroscopies. It will be shown that both the length and the substitution of the oligomers have a marked effect on their ultrafast excited-state dynamics.

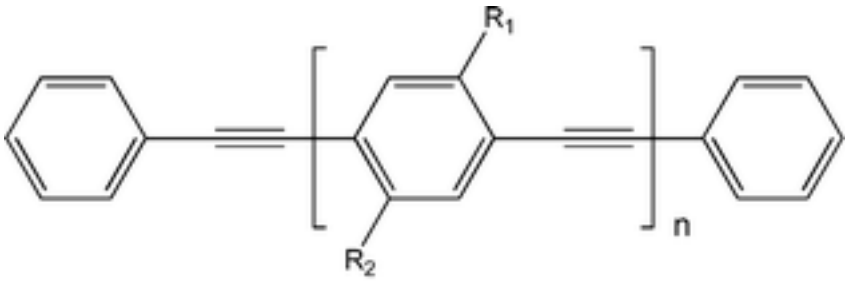

O5: n = 4, $R_1 = C_{12}H_{25}$, R_2 = H
O7: n = 6, $R_1 = C_{12}H_{25}$, R_2 = H
O9: n = 8, $R_1 = C_{12}H_{25}$, R_2 = H
O17: n = 16, $R_1 = C_{12}H_{25}$, R_2 = H
O5b: n = 4, $R_1 = R_2 = OC_{12}H_{25}$

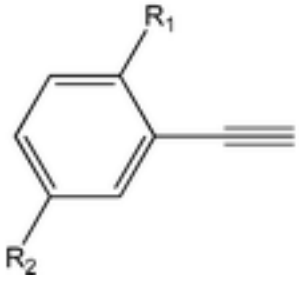

MePE: $R_1 = CH_3$, R_2 = H
MoPE: $R_1 = R_2 = OCH_3$

Fig. 1 Structure of the OPEs and of the monomeric units.

Experimental

Synthesis

All air- or water-sensitive reactions were carried out under argon. Solvents were generally dried and distilled prior to use. Reactions were monitored by thin-layer chromatography (TLC) on Merck silica gel 60 F_{254} (0.2 mm) precoated aluminium foils. Reaction products were separated by flash chromatography (FC) on Merck silica gel 60 (0.040–0.063 mm, 230–400 mesh), except otherwise noted. ^{1}H NMR: Bruker Avance DPX360 (^{1}H 300.14 MHz), or Bruker Avance DRX500 (^{1}H 500.13 MHz) in $CDCl_3$ solutions unless otherwise stated, chemical shifts (δ) are given in parts per million relative to $Si(CH_3)_4$ as internal standard, and *J* values are in hertz. Assignments are based on homonuclear COSY-45, ^{1}H{^{1}H} NOE difference correlations, and/or chemical shifts. Mass spectra: Vacuum Generators Micromass 7070E instrument equipped with a data system DS 11-250. ES$^+$-MS (electrospray ionization, positive mode) using dithranol as matrix. MALDI-MS (matrix assisted laser desorption ionization), using dithranol, DHB (2,5-dihydroxybenzoic acid) or DCTB (2-[(2*E*)-3-(4-*ter*-butylphenyl)-2-methylprop-2-enylidene]malonitrile) dissolved in $CHCl_3$ (0.05 M) as matrix (dried droplet method) and averaging 200–1100 shots.

2-Dodecyl-4-phenylene-containing oligomers (**O5**–**17**) were prepared from 3,3-diethyl-1-[3-dodecyl-4-[(trimethylsilyl) ethynyl]phenyl]-1-triazene[19] according to the methodology reported

in the literature.[19,20]

O5. The corresponding 4-ethynyl pentamer (42 mg, 36 μmol) was reacted with iodobenzene (7.3 mg, 36 μmol) in THF (2 ml) and *N*,*N*-diisopropylethylamine (25 μl, 143 μmol) and in the presence of Pd_2dba_3 (0.6 mg, 0.7 μmol), triphenylphosphine (0.5 mg, 1.8 μmol) and CuI (0.1 mg, 0.7 μmol) at 60 °C for 16 h. The crude product was purified by FC (hexane–Et_2O, 9 : 1) to yield 20 mg (45%) of **O5** as a yellow solid. ^{1}H NMR (500.13 MHz): δ 0.87 (m, 12H), 1.27 (m, 56H), 1.35 (m, 8H), 1.42 (m, 8H), 1.72 (m, 8H), 2.85 (m, 8H), 7.32–7.42 (m, 14H), 7.46–7.50 (m, 4H), 7.52–7.55 (m, 4H). HRMS (MALDI) (DHB): 1250.95; calcd average mass for $C_{94}H_{122}$ = 1250.95.

O7. The corresponding 4-ethynyl heptamer (176 mg, 103 μmol) was reacted with iodobenzene (21 mg, 103 μmol) as described for **O5** to yield 84 mg (46%) of **O7** as a yellow glassy solid. ^{1}H NMR (500.13 MHz): δ 0.87 (m, 18H), 1.27 (m, 84H), 1.35 (m, 12H), 1.42 (m, 12H), 1.73 (m, 12H), 2.86 (m, 12H), 7.32–7.42 (m, 18H), 7.46–7.50 (m, 6H), 7.52–7.55 (m, 4H). HRMS (MALDI) (DHB): 1787.39; calcd average mass for $C_{134}H_{178}$ = 1787.39.

O9. The corresponding 4-iodononamer (240 mg, 102 μmol) was reacted with phenylacetylene (34 μl, 306 μmol), as described for **O5** to yield 16 mg (7%) of **O9** as a yellow solid. ^{1}H NMR (500.13 MHz): δ 0.87 (m, 24H), 1.27 (m, 112H), 1.35 (m, 16H), 1.42 (m, 16H), 1.72 (m, 16H), 2.86 (m, 16H), 7.32–7.42 (m, 22H), 7.46–7.50 (m, 8H), 7.52–7.55 (m, 4H). HRMS (MALDI) (dithranol): 2323.85; calcd average mass for $C_{174}H_{234}$ = 2323.83.

O17. The corresponding 4-iodoheptadecamer (35.2 mg, 8 μmol) was reacted with phenylacetylene (2.6 μl, 24 μmol) as described for **O5** to yield 6.8 mg (19%) of **O17** as a yellow solid. ^{1}H NMR (500.13 MHz): δ 0.87 (m, 48H), 1.27 (m, 224H), 1.35 (m, 32H), 1.42 (m, 32H), 1.73 (m, 32H), 2.86 (m, 32H), 7.32–7.40 (m, 38H), 7.46–7.55 (m, 20H). Anal. Calcd for $C_{334}H_{458}$ (4473.37): C, 89.68; H, 10.32. Found: C, 89.46; H, 10.78.

2,5-Didodecanoxy-4-phenylene-containing OPE (O5b). A solution of 67 mg (44 μmol) of the corresponding tetramer, which was prepared following the procedure given in ref. 21 was reacted with 30.0 mg (44 μmol) of 2,5-dodecanoxy-4-iodo-1-(phenylethynyl)benzene[22] in THF–NEt_3 (12 ml, 5 : 1) in the presence of $Pd(PPh_3)_2Cl_2$ (3.1 mg, 4.4 μmol) and CuI (0.8 mg, 4.4 μmol) at 50 °C for 16 h. The crude product was purified by FC (toluene–hexane 1 : 1) to yield 23.0 mg (25%) of a yellow solid. ^{1}H NMR (500.13 MHz): δ 0.86 (m, 24H), 1.25 (m, 112H), 1.36 (m, 16H), 1.51 (m, 16H), 1.85 (m, 16H), 4.02 (m, 16H), 7.00–7.02 (m, 8H), 7.35 (m, 6H), 7.53 (m, 4H). HRMS (MALDI) (DHB): 2051.66; calcd average mass for $C_{142}H_{218}O_8$ = 2051.66.

Samples

The solvents, toluene and paraffin oil (100–200 mPa s) were of the highest commercially available purity and were used as received. For time-correlated single-photon counting

measurements, the sample solutions were contained in a 1 cm quartz cell and their absorbance at the excitation wavelength was around 0.1. For fluorescence up-conversion measurements, the sample solutions were enclosed in a 0.4 mm rotating cell and their absorbance at 400 nm was about 0.1. For transient absorption, the solutions were in a 1 mm thick quartz cell, had an absorbance around 0.5 at 400 nm and were continuously stirred by N_2-bubbling. For the other experiments, aerated solutions were used. No significant sample degradation was observed after the measurements.

Time-resolved fluorescence measurements

The time-correlated single-photon counting (TCSPC) setup used to perform the time-resolved fluorescence measurements on nanosecond time-scale has been described in detail elsewhere.[23] Excitation was carried out at 395 nm and the detected fluorescence wavelength was selected with interference filters. The full width at half maximum (FWHM) of the instrument response function (IRF) was around 200 ps.
Excited-state lifetime measurements on shorter time-scales were performed using fluorescence up-conversion (FU). The experimental setup has been described in detail elsewhere.[24] Excitation was achieved at 400 nm with the frequency-doubled output of a Kerr lens mode-locked Ti:Sapphire laser (Tsunami, Spectra-Physics). The output pulses, centred at 800 nm, had a duration of 100 fs and a repetition rate of 82 MHz. The polarization of the pump beam was at the magic angle relative to that of the gate pulses at 800 nm. The FWHM of the IRF was *ca.* 210 fs.

Transient absorption (TA) measurements

Excitation was done at 400 nm using the frequency-doubled output of a standard 1 kHz amplified Ti:Sapphire system (Spectra-Physics). Probing was achieved with a white light continuum obtained by focusing 800 nm pulses in a H_2O–D_2O mixture. The probe beam was split before the sample into a pumped signal beam and an unpumped reference beam. The transmitted signal and reference beams were detected with two ORIEL Multispec 125 spectrographs coupled to 2048 pixels CCD lines (Entwicklungsbüro G. Stresing, Berlin). To improve sensitivity, the pump light was chopped at half the amplifier frequency, and the transmitted signal intensity was recorded shot by shot. It was corrected for intensity fluctuations using the reference beam. The transient spectra were averaged until the desired signal-to-noise ratio was achieved.

Data analysis

The time profiles were analyzed by iterative reconvolution of the instrument response function with trial functions (sum of exponentials) using a nonlinear least squares fitting procedure (MATLAB, The MathWorks, Inc.).

Quantum chemistry calculations

The ground-state gas phase geometries of monomeric PE units (Fig. 1) and analogues of **O5** and **O5b** but with $n = 2$ and $R_1 = R_2 = CH_3$ and OCH_3, respectively, were fully optimized at the

density functional level of theory (DFT) using the BP86 functional,[25] and a [3s2p1d] basis set.[26] Transition dipole moments were computed using time-dependent density functional theory (TDDFT),[27] with the same functional and basis set. The calculations were carried out using Turbomole version 5.8.0.[28,29]

Results and discussion

Steady-state measurements

The steady-state absorption and fluorescence spectra of **O5**, **O17** and **O5b** in toluene are depicted in Fig. 2. Compared to that of **O5** the absorption band of **O17** is red shifted and markedly broader. The absorption bands of **O7** and **O9** have a shape similar to that of **O17** and their maxima, λ_{abs}, are slightly blue shifted (see Table 1). The broadening of the absorption band with increasing OPE length can be explained in terms of an increased torsional disorder.[15] The fluorescence band of **O5**–**17** is narrow and exhibits a vibronic band whose relative intensity decreases with increasing oligomer length. The red shift of the fluorescence maximum, λ_{fl}, with increasing number of PE units up to $N \simeq 10$ is also consistent with that observed with similar OPEs.[10] The absorption and fluorescence spectra of the alkoxy-substituted OPE, **O5b**, resemble those of **O5**–**17**. However, the band maxima of **O5b** are red-shifted by about 3200 cm^{-1} relatively to those of **O5**.

Table 1 Spectroscopic and photophysical parameters relevant to the OPEs in toluene (limit of error on Φ_{fl}: ±0.02 and on τ_{fl}: ±2%)

OPE	λ^{abs}/nm	λ^{fl}/nm	Φ^{fl}	τ^{fl}/ps	k_{rad}/ns^{-1}	f[a]	M[b]/D
O5	365	404	0.91	500	2.0	1.93	13.4
O7	369	412	0.90	450	2.3	2.22	14.4
O9	377	414	0.93	350	2.6	2.53	15.4
O17	376	414	0.91	355	2.5	2.43	15.1
O5b	414	461	0.80	850	0.94	1.15	11.0

[a] f = oscillator strength. [b] M = transition dipole moment.

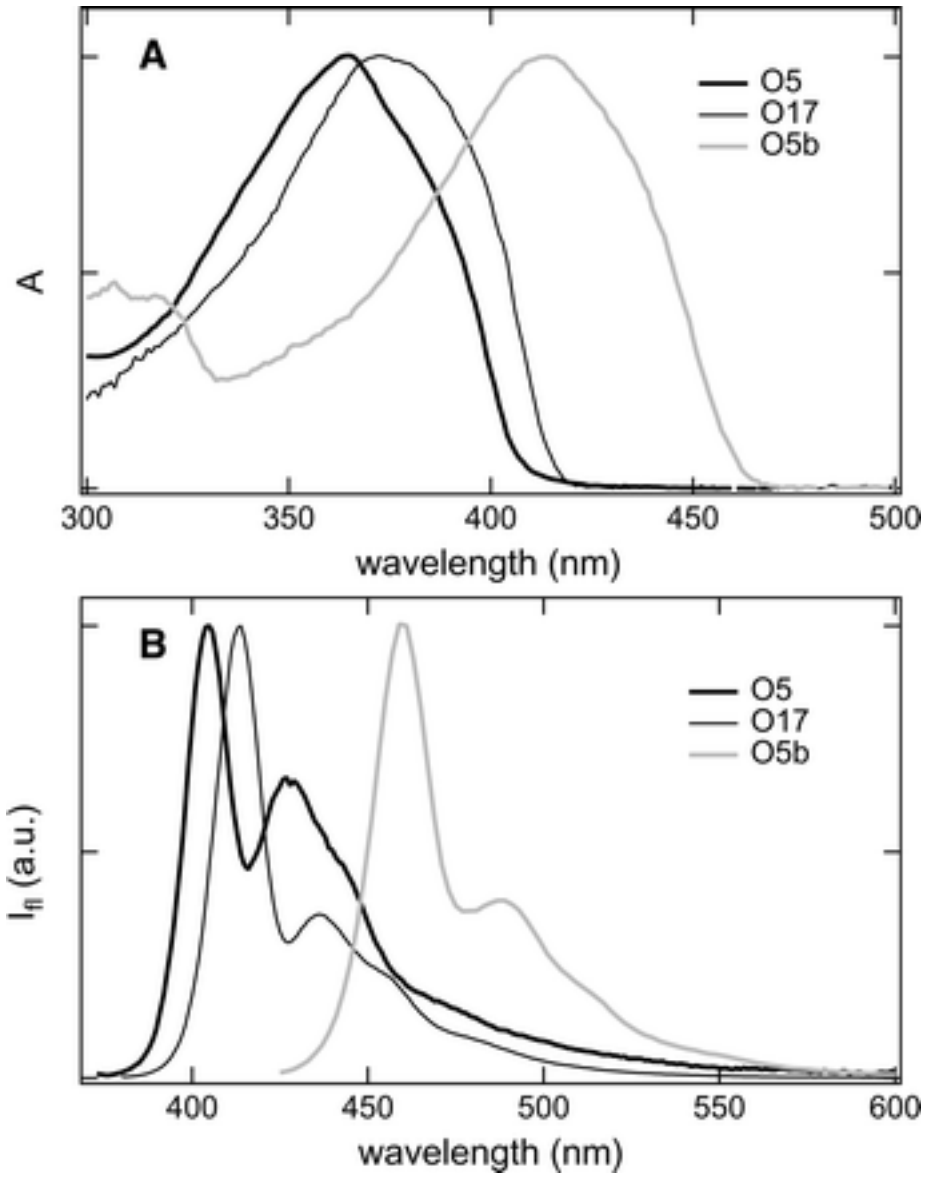

Fig. 2 Absorption (A) and emission (B) spectra of OPEs in toluene.

The fluorescence quantum yield, Φ_{fl}, of all five oligomers, determined using perylene in toluene as standard (Φ_{fl} = 0.94),[30] are listed in Table 1. The fluorescence quantum yields of the alkyl-substituted OPEs are essentially all around 0.9, while that of the alkoxy-substituted OPE is noticeably smaller.

TCSPC measurements

The fluorescence decays of all five oligomers measured around 420 nm (**O5**–**17**) and 450 nm (**O5b**) could be very well reproduced by the convolution of the IRF with a single exponential function. Table 1 reveals that the fluorescence lifetime, τ_{fl}, of alkyl-substituted OPEs exhibits a nearly continuous decrease up to N = 9 and then remains essentially constant. The fluorescence lifetime of 590 ps, measured with an unsubstituted OPE with N = 2,[31] correlates very well with the dependence found here. Moreover, a lifetime of ~350 ps has been reported with an OPE with N = 9, but with shorter alkyl-substituents ($R_1 = R_2 = C_6H_{13}$).[13] The excellent agreement with the value measured here with **O9** indicates that alkyl-substitution has essentially no effect

on the excited-state properties of OPEs.
The situation is different with alkoxy-substitution, which leads not only to a decrease of the excited-state energy (see Fig. 2) but also to a increase of τ_{fl}, the fluorescence lifetime of **O5b** being almost twice as large as that of **O5**.
Information on the origin of the measured variation of the fluorescence lifetime can be obtained by calculating the radiative rate constant, $k_{rad} = \Phi_{fl}\tau^{-1}_{fl}$, and the rate constant of non-radiative deactivation, $k_{nr} = \tau^{-1}_{fl} - k_{rad}$. From these calculations, it appears that, while k_{nr} is essentially the same for all compounds, k_{nr} = 0.2–0.35 ns^{-1}, k_{rad} increases continuously from **O5** to **O9** and then remains constant at a value of ~2.6 ns^{-1} for larger *N*. The radiative rate constant calculated for the above-mentioned oligomer with *N* = 2,[31] amounts to 1.54 ns^{-1} and correlates very well with the length dependence found here. These calculations also reveal that the longer fluorescence lifetime of **O5b** originates from a smaller k_{rad} value.

A further insight can be gained by considering the oscillator strength, *f*, and the length of the transition dipole moment, *M*, associated with the S_1–S_0 transition,

$$f = \frac{\varepsilon_0 c^3 m_e}{2\pi e^2 \nu_{av}^2 f(n)} k_{rad} \quad (1)$$

$$M^2 = \frac{3\varepsilon_0 hc^3}{16\pi^3 f(n)\nu_{av}^3} k_{rad} \quad (2)$$

where ε_0 is the vacuum permittivity, *c* the speed of light, m_e the mass of the electron, *e* the elementary charge, $f(n) = n[(n^2 + 2)/3]^2$, *n* being the refractive index, and ν_{av} the average frequency.[32]

The length dependence observed with k_{rad} is of course also present with *f* and *M* (see Table 1). However, it is interesting to note that for the alkyl-substituted OPEs, *f* is substantially larger than unity. This is a clear indication that the OPEs can be described as ensembles of coherently coupled chromophores, whose collective fluorescence can be considered as superradiance.[33] The increase of *f* and *M* with *N* stops around $N \simeq 10$, in agreement with the shift of the fluorescence spectrum with oligomer length. The oscillator strength of **O5b** is substantially smaller than that of **O5**, which has the same *N*. Quantum chemical calculations on the monomeric units, MePE and MoPE (see Fig. 1), predict a dipole moment of 4.0 D and 2.4 D for the first electronic transition of MePE and MoPE, respectively. It is thus reasonable to assume that this difference should also exist in the oligomers, as their transition dipole can be viewed as resulting from the excitonic interaction between the monomeric units.

FU and TA measurements in toluene

Fig. 3A and B show the time profiles of the early fluorescence of **O5** and **O5b** in toluene

recorded near the band maximum. The rise of the intensity with **O5** is essentially prompt, except for a small component with a relative amplitude of 0.05 and a time constant around 3.5 ps. The early fluorescence dynamics of **O9** and **O17** in toluene was also investigated and was found to be rather similar to that of **O5**, *i.e.* the rise consists in a large prompt component and in two weak components with time constants around 2–4 ps and 20–40 ps (see Table 2). Apart from small differences in the amplitudes, no significant wavelength dependence of the fluorescence dynamics could be found with **O5**–**17** between 415 and 550 nm. This indicates that, in this range, the fluorescence bandshape of these OPEs does not change considerably with time. A qualitatively similar behaviour has been reported for an OPE with $N = 9$, except on the blue side of the emission band, where a 60 ps decay component, corresponding to a collapse of the blue edge of the band, was observed.[13] The time resolution of these measurements was however not sufficient to observe faster dynamic feature. Measurements at wavelengths shorter than 420 nm could not be performed here because of the proximity of the excitation (400 nm).

Table 2 Time constants and amplitudes associated with the early fluorescence dynamics of the OPEs measured in toluene near the band maximum (limit of error on the lifetimes: ±5%; a negative amplitude indicates a rising component)

OPE	τ_1/ps	A_1	τ_2/ps	A_2
O5	3.5	–0.05	—	—
O9	3.7	–0.03	35	–0.06
O17	1.5	–0.03	15	–0.07
O5b	1.2	–0.3	43	–0.3

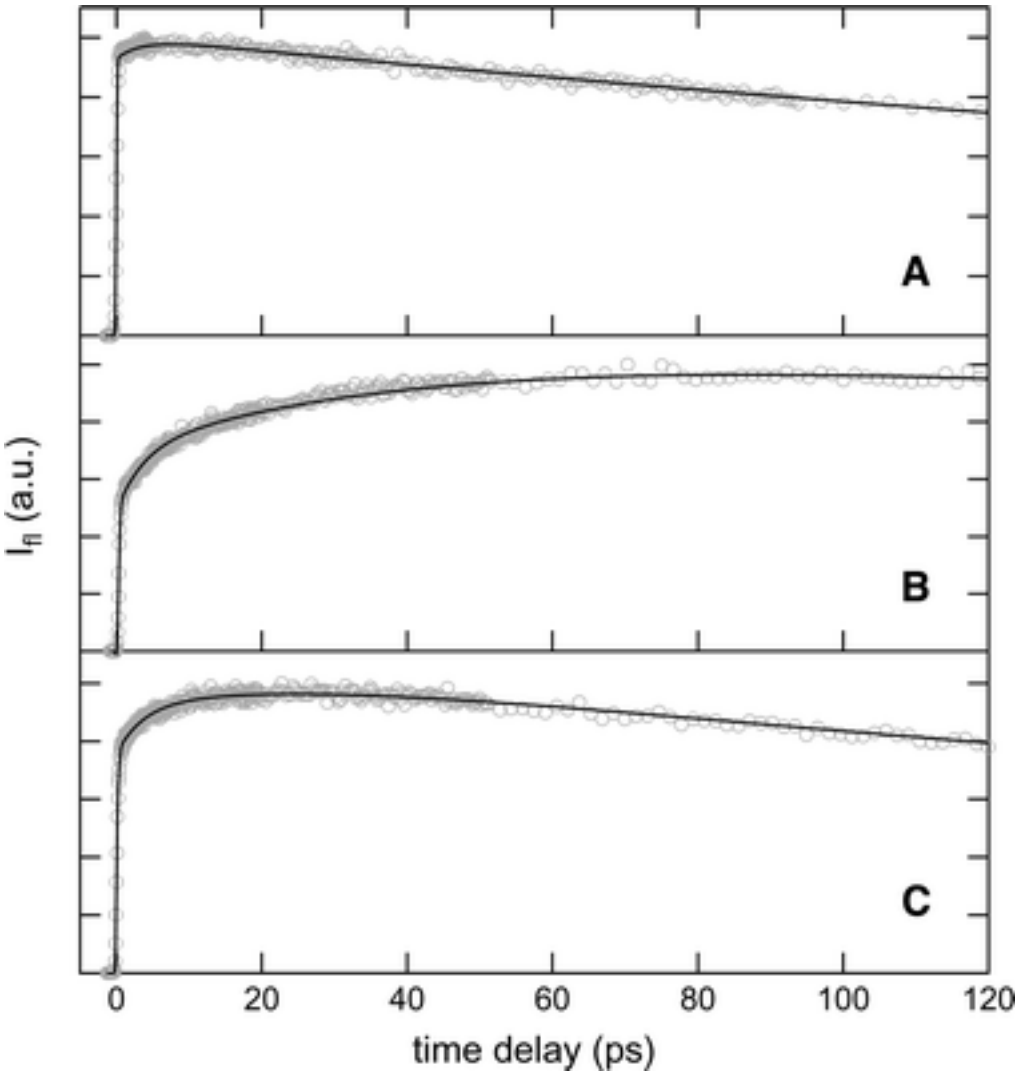

Fig. 3 Fluorescence time profiles recorded in toluene: (A) **O5** at 425 nm, (B), **O5b** at 435 nm, (C) **O5b** at 420 nm.

The rise of the FU signal measured with **O5b** is clearly different (Fig. 3B): 40% are prompt, and the remaining is biphasic with time constants of 1.2 and 43 ps (see Table 2). The time profiles measured between 450 and 615 nm are all very similar, except for small differences in the amplitude of the various components. At 420 nm however, *i.e.* at the very blue edge of the band, the time profile differs substantially as it exhibits a fast decaying component with a time constant of 240 ps additionally to the 850 ps component (Fig. 3C). This feature can also be interpreted as a collapse of the blue side of the fluorescence spectrum.

TA spectra recorded with **O5** in toluene upon 400 nm excitation are depicted in Fig. 4A. The negative band below 500 nm resembles very much the red part of the fluorescence spectrum and is due to stimulated emission. The time profile of the spectral area between 425 and 485 nm is very similar to that measured by FU, *i.e.* exhibits a weak 3–4 ps rising component and a 500 ps decay. Fig. 4B shows intensity-normalized spectra in this spectral region recorded at several time delays. The most intense peak corresponds to the first vibronic band observed in the steady-state spectrum (Fig. 2), while the smaller one can only be seen as a shoulder in the steady-state spectrum. According to these figures, the fluorescence spectrum is more structured at early time and becomes similar to the stationary spectrum after about 20–30 ps. This change is too small to be detected in the FU measurements. This feature could be interpreted in terms

of structural relaxation in the S_1 state. It has been shown that the intensity of the vibronic transition of these OPEs changes significantly with the degree of torsion in the molecule, the vibronic side-bands being more intense as the molecule deviates from planarity.[15] Therefore, the changes shown in Fig. 4B could be associated to the relaxation from the non-planar Franck–Condon (FC) region to the planar equilibrium region of the S_1 state.

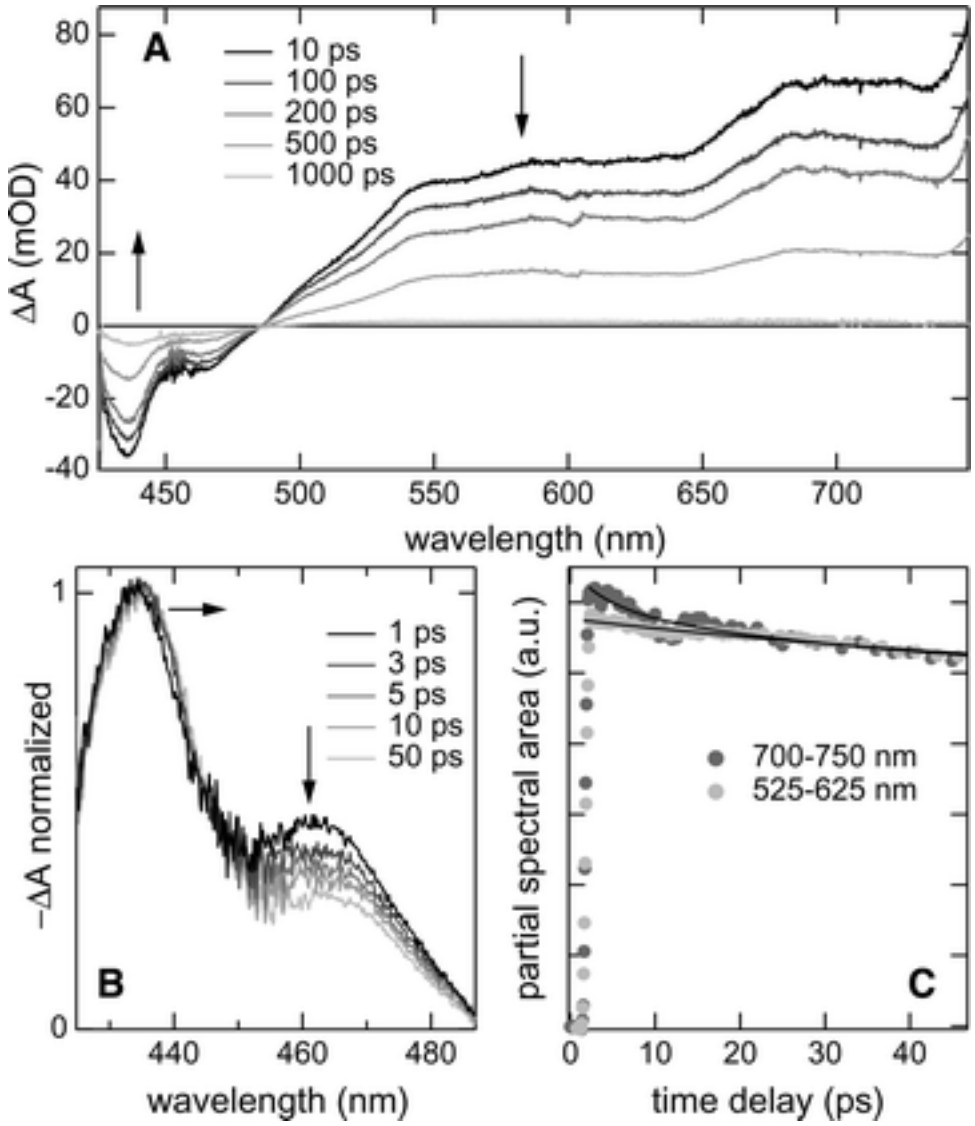

Fig. 4 (A) Transient absorption spectra recorded with **O5** in toluene at different time delays after excitation, (B) intensity-normalised transient spectra in the stimulated emission region, (C) time dependence of the area in two spectral regions.

The TA spectra above 500 nm can be assigned to excited-state absorption (ESA). The ESA spectrum is very broad and structureless. The time dependence of the spectral area between 525 and 625 nm can be well reproduced using a single exponential function with a time constant of about 500 ps, as found by time-resolved fluorescence (Fig. 4C). On the other hand, the time dependence of the spectral area between 700 and 750 nm is biphasic with a 500 ps component and an additional decaying component with a time constant of about 3–4 ps. This time constant matches well that associated with the small rising component of the fluorescence and must thus

originate from the same process, most probably structural rearrangement of the molecule in the S_1 state. It can thus be concluded that the absorption cross-section of the unrelaxed S_1 state above 700 nm is larger than that of the relaxed state. On the contrary, the radiative rate constant of the FC S_1 state is apparently slightly smaller than that of the relaxed state, hence the small initial rise of the fluorescence intensity.

The small rising components of the fluorescence measured with **O9** and **O17** is also most probably due to structural relaxation in the excited state. The biphasic nature of the rise observed with these longer OPEs could originate from a distribution of time constants. It is indeed well known that kinetics resulting from a distribution of time constants with a Gaussian distribution of amplitudes can be well reproduced with a biexponential function.[34–36] Such distribution is reasonable as the length of the OPE, hence the number of possible conformations, increases.

Fig. 5A shows TA spectra recorded upon excitation of **O5b** in toluene. Similarly to those of **O5**, they consist in stimulated emission at short wavelength and in ESA above 550 nm. The time profile of the spectral area between 440 and 550 nm is essentially the same as the fluorescence time profile measured by FU above 450 nm. However, Fig. 5B reveals a substantial time dependence of the stimulated fluorescence spectrum. It is first broad, structureless, and not very different from the mirror image of the absorption band. As time proceeds, the blue side of the band narrows and a vibrational structure appears. After about 200–300 ps, the spectrum is essentially the same as the steady-state spectrum. The large spectral dynamics on the blue edge is in good agreement with the fast decay measured by FU at 420 nm (Fig. 3C). The changes taking place on the red edge of the spectrum, i.e. above about 520 nm have to be considered with caution as they may be due to an underlying contribution of the broad ESA band. The other spectral changes are too small to appear in the FU measurements.

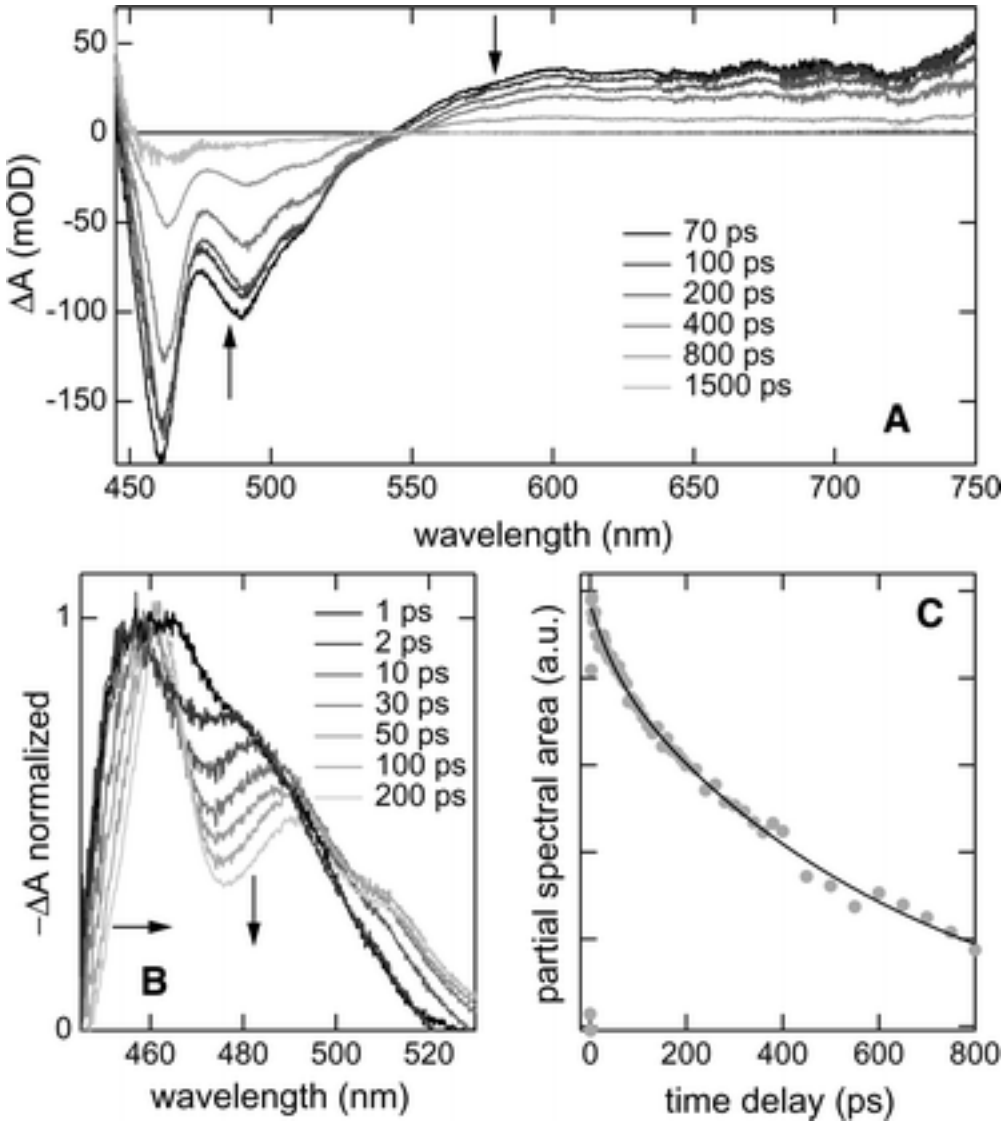

Fig. 5 (A) Transient absorption spectra recorded with **O5b** in toluene at different time delays after excitation, (B) intensity-normalised transient spectra in the stimulated emission region, (C) time dependence of the spectral area between 600 and 670 nm.

The red part of the TA spectrum exhibits a very broad and structureless ESA, which resembles the ESA spectrum of **O5** (Fig. 4A). The time profile of the transient absorption in this region is independent of the wavelength. As illustrated in Fig. 5C, the time dependence of the spectral area between 600 and 750 nm is biphasic and can be well reproduced with a biexponential function with 30 and 850 ps time constants. The slower component can thus be ascribed to the decay of the relaxed S_1 state, while the fast one is most probably due to relaxation from the FC region of the S_1 state.

The main difference between the excited-state dynamics of the alkyl- and the alkoxy-substituted OPEs lies in the rise of the fluorescence intensity. Indeed, with the first, 90% of the rise is prompt, while only 40% is prompt with the latter. A larger torsional disorder of **O5b** in the ground state cannot be invoked to account for such a difference. Indeed, if this were the case, the absorption spectrum of **O5b** would be considerably broader than that of **O5**, contrary to the observation. Moreover, DFT calculations of the ground-state geometry of models of **O5**

and **O5b**, with $n = 2$ and with $R_1 = R_2 = CH_3$ and OCH_3, respectively, have been undertaken to find out whether alkoxy-substitution has an influence on the strength of the bond connecting the phenylene moieties. These calculations reveal that this bond has a length of 1.54 Å, independently of the nature of the substituent. It has thus a single bond character, and consequently the barrier to rotation about the long axis of the oligomer, hence the torsional disorder should be essentially the same for both OPEs.

We suggest that the difference observed between **O5** and **O5b** can be qualitatively discussed in terms of the excitonic nature of the S_1 state. As mentioned above, the transition dipole moment of these OPEs can be viewed as resulting from the interaction of the transition dipoles of the individual PE units. In the case of **O5**, the transition dipole moment is independent of the degree of torsional disorder, as the transition dipole moment of each MePE unit is aligned along the long axis of the molecule (see Fig. 6A). In this case, the interaction between the transition dipoles of the monomeric units is essentially the same in both non-planar and planar geometries. The situation is different for **O5b** as the S_0–S_1 transition dipole moment of MoPE has been calculated to be not only smaller than that of MePE but to make an angle of about 30° relatively to the long axis of the molecule, defined by the triple bond. As a consequence, the transition dipole moment of **O5b** should depend substantially on torsion as illustrated in Fig. 6B. If this molecule is torsionally disordered, the short-axis components of the individual transition dipoles are randomly oriented and thus cancel. Therefore, only the long-axis components contribute to the total dipole moment. On the other hand, if **O5b** is planar, both long- and short-axis components interact and the total dipole moment, hence the oscillator strength, is larger than in the previous case. This effect is only valid for the planar geometry of **O5b** where all the R_1-substituents are on one side, and the R_2 substituents on the other side. Of course, a planar configuration, where the side at which the substituents are located is alternating is also possible. In this geometry, the short-axis components of the monomeric transition dipoles would cancel as in the torsional disordered configuration. However, considering the bulkiness of the substituents, such planar alternating geometry is strongly disfavoured by steric hindrance relatively to the other.

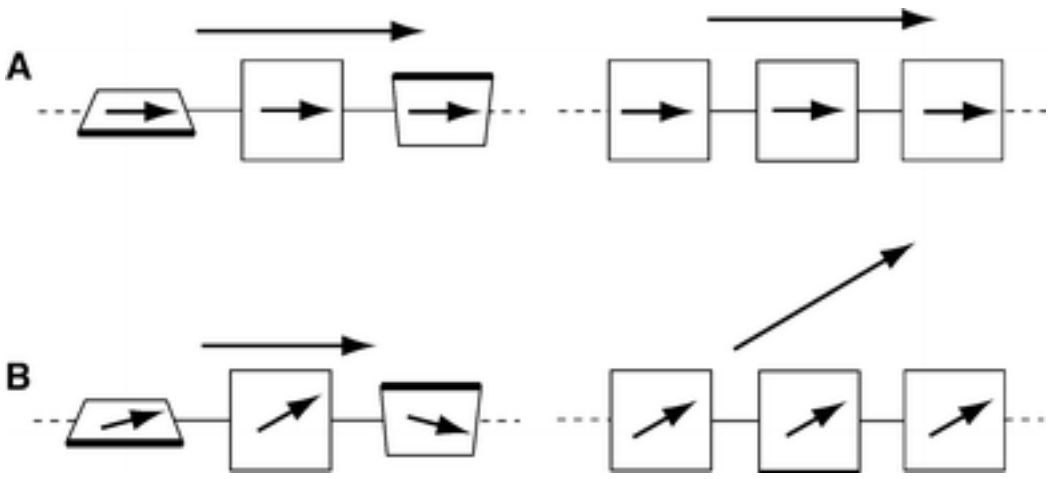

Fig. 6 Schematic representation of the exciton model for (A) **O5** and (B) **O5b**. The small arrows are the transition dipole moments of the monomeric units while the long arrows represent the transition dipole moment of the oligomers.

This crude model can explain why planarization in the S_1 state results in a small rising component of the fluorescence intensity with alkyl-substituted OPEs (Fig. 3A) and conversely in an important rising component with the alkoxy-substituted OPE (Fig. 3B). This model also predicts that, if the alkoxy-substituents were in *meta*-position to each other, the oscillator strength of the OPE would no longer depend on the torsional disorder, as the transition dipole moments of the monomeric units would be fully aligned along the long axis.

To further confirm that the early dynamic features found with **O5b** are indeed associated with structural relaxation in the S_1 state, **O5** and **O5b** have also been investigated in a highly viscous solvent, namely in paraffin oil. Fig. 7A shows that the absorption spectra of **O5b** in toluene and paraffin oil are almost identical, while the fluorescence spectra differ substantially. The fluorescence spectrum in paraffin oil is very similar to the stimulated emission spectrum measured at early time in toluene (Fig. 5B). It is indeed less structured and broader on the blue side than the steady-state spectrum in toluene. This indicates that, in paraffin oil, the structural changes directly after excitation have been slowed down to a time-scale similar or longer than that of the S_1 population decay. Therefore, emission in this viscous medium takes place from an excited-state population in partial torsional disorder. This assumption is supported by Fig. 7B that shows the time profile of the fluorescence intensity measured with **O5b** in paraffin oil at the band maximum. In this solvent, more than 90% of the fluorescence intensity rise promptly and only a weak 20–25 ps component can be observed. This weak component could also be related to structural rearrangement but does probably not involve large amplitude motion.

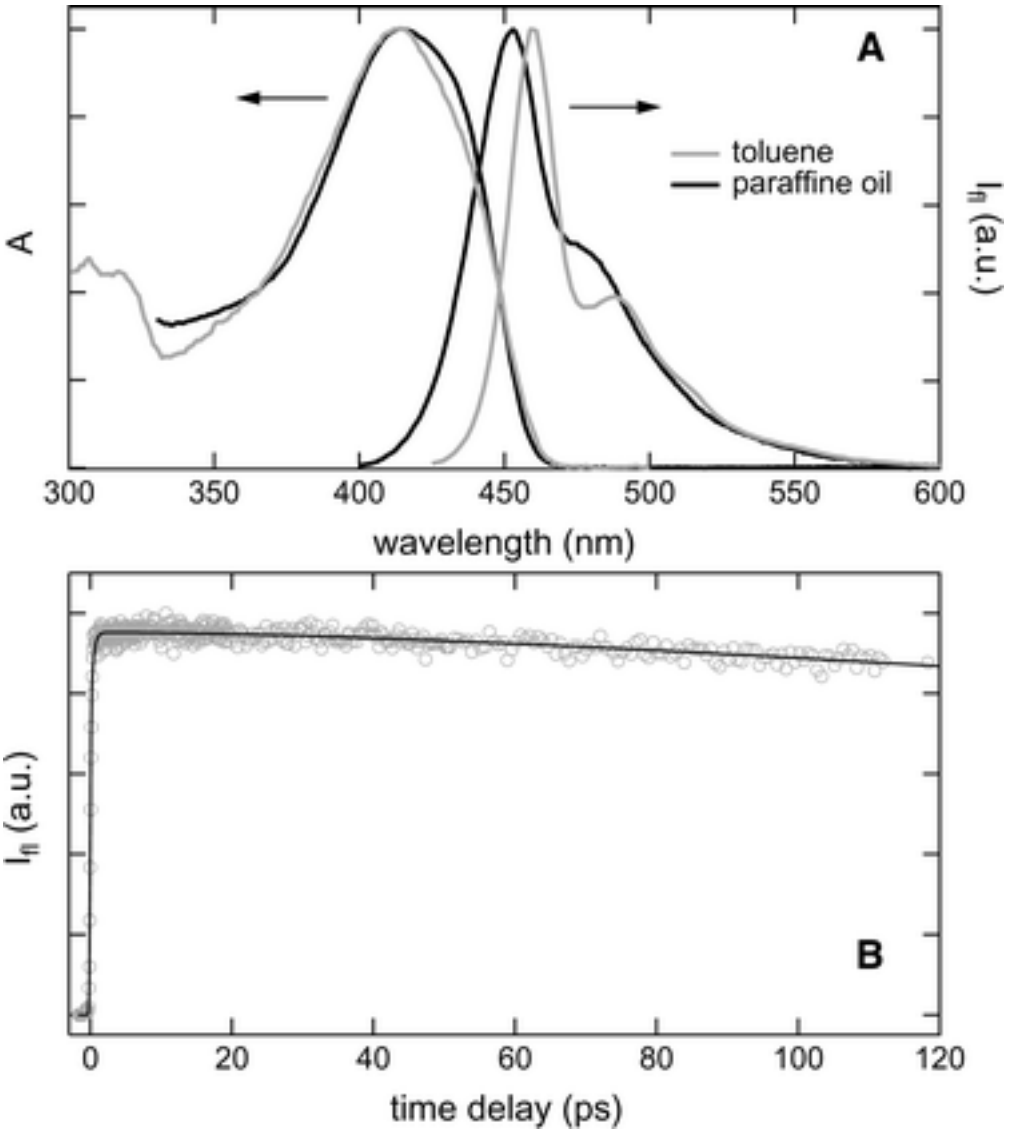

Fig. 7 (A) Fluorescence spectrum of **O5b** in toluene and paraffin oil, (B) fluorescence time profile of **O5b** at 450 nm in paraffin oil.

The fluorescence quantum yield of **O5b** in paraffin oil is reduced by a factor of three relatively to toluene, while that of **O5** decreases by less than 5%. Moreover, the small 3–4 ps rising component observed with **O5** in toluene is totally absent in paraffin oil, *i.e.* the rise of the whole fluorescence intensity is prompt. This is a further confirmation that the oscillator strengths for the fluorescence of **O5** and **O5b** have very different dependence on torsion. Finally it should be noted that the rise of the fluorescence intensity and the collapse of the blue edge of the fluorescence band of **O5b** are associated with different time constants. This is most certainly due to the fact that the structural changes occurring after photoexcitation involve several torsional coordinates, which relax on different time-scales and which have a different influence on the shape and intensity of the fluorescence spectrum.

Concluding remarks

It has been known for a long time that both the length and the nature of the substitution can have a substantial effect the spectral properties of OPEs. In this investigation, we have shown that these two parameters can also have a major influence on their excited-state dynamics. The

S_1 lifetime can be almost halved by increasing the number of PE units from 2 to 9. Moreover, replacing alkyl- by alkoxy substituents not only leads to an increase of the excited-state lifetime but also to substantial differences in the early fluorescence dynamics and in the viscosity dependence of the fluorescence quantum yield. The results indicate that the oscillator strength of the alkoxy-substituted OPE decreases strongly as the molecule departs from planarity. Therefore, the structural relaxation occurring directly after population of the S_1 state can be easily observed by monitoring the fluorescence dynamics. For the same reason, the fluorescence quantum yield of this OPE is strongly reduced in viscous media. All these effects can be qualitatively understood with a simple excitonic model, where the OPEs are considered as linear arrays of coherently coupled PEs. It is clear that a more quantitative description requires a more sophisticated treatment of the coupling between the PE units.[3]
Knowledge of the excited-state dynamics of OPEs is particularly important for photonic applications. In a forthcoming paper, we will show that these compounds can act as both spacer and active chromophore for long-distance excitation energy transfer.

Acknowledgements

This work was supported by the Fonds National Suisse de la Recherche Scientifique through projects 200020-107466 and 200020-109461.

References

1 A. Kraft, A. C. Grimsdale and A. B. Holmes, Electroluminescent conjugated polymers - Seeing polymers in a new light, *Angew. Chem., Int. Ed.*, 1998, **37**, 402–408 [Links].

2 J.-L. Brédas, D. Beljonne, V. Coropceanu and J. Cornil, Charge-transfer and energy-transfer processes in π-conjugated oligomers and polymers: a molecular picture, *Chem. Rev.*, 2004, **104**, 4971–5003 [Links].

3 W. Barford, *Electronic and optical properties of conjugated polymers*, Oxford University Press, New York, 2005.

4 R. Giesa, Synthesis and properties of conjugated poly(aryleneethynylene)s, *J. Macromol. Sci. Rev. Macrol. Chem. Phys.*, 1996, **C36**, 631–670.

5 U. H. F. Bunz, Poly(aryleneethynylene)s: syntheses, properties, structures, and applications, *Chem. Rev.*, 2000, **100**, 1605–1644 [Links].

6 J. M. Tour, Molecular electronics. Synthesis and testing of components, *Acc. Chem. Res.*, 2000, **33**, 791–804 [Links].

7 A. Morandeira, E. Vauthey, A. Schuwey and A. Gossauer, Ultrafast excited state dynamics of tri- and hexaporphyrin arrays, *J. Phys. Chem. A*, 2004, **108**, 5741–5751 [Links].

8 J. N. Clifford, T. Gu, J.-F. Nierengarten and N. Armaroli, Photoinduced energy and electron transfer in fullerene–oligophenyleneethynylene systems: dependence on the substituents of the oligomer unit, *Photochem. Photobiol. Sci.*, 2006, **5**, 1165–1172 [Links].

9 J. Wiberg, L. Guo, K. Petterson, D. Nilsson, T. Ljungdahl, J. Mårtensson and B. Albinsson, Charge recombination *versus* charge separation in donor–bridge–acceptor systems, *J. Am. Chem. Soc.*, 2007, **129**, 155–163 [Links].

10 H. Meier, D. Ickenroth, U. Stalmach, K. Koynooov, A. Bahtiar and C. Bubeck, Preparation and nonlinear optics of monodisperse oligo(1,4-phenyleneethynylene)s, *Eur. J. Org. Chem.*, 2001, 4431–4443 [Links].

11 R. Kopelman, M. Shortreed, Z.-Y. Shi, W. Tan, Z. Xu, J. S. Moore, A. Bar-Haim and J. Klafter, Spectroscopic evidence for excitonic localisation in fractal antenna supermolecules, *Phys. Rev. Lett.*, 1997, **78**, 1239–1242 [Links].

12 V. D. Kleiman, J. S. Melinger and D. McMorrow, Ultrafast dynamics of electronic excitations in a light-harvesting phenylacetylene dendrimer, *J. Phys. Chem. B*, 2001, **105**, 5595–5598 [Links].

13 M. I. Sluch, A. Godt, U. H. F. Bunz and M. A. Berg, Excited-state dynamics of oligo(*p*-phenyleneethynylene): quadratic coupling and torsional motions, *J. Am. Chem. Soc.*, 2001, **123**, 6447–6448 [Links].

14 A. Beeby, K. S. Findlay, P. J. Low, T. B. Marder, P. Matousek, A. W. Parker, S. R. Rutter and M. Towrie, Studies of the S1 state in a prototypical molecular wire using picosecond time-resolved spectroscopies, *Chem. Commun.*, 2003, 2406–2407 [Links].

15 L. T. Liu, D. J. Yaron, M. I. Sluch and M. A. Berg, Modelling the effect of torsional disorder on the spectra of poly- and oligo-(*p*-phenyleneethylenes), *J. Phys. Chem. B*, 2006, **110**, 18844–18852 [Links].

16 S. Tretiak, V. Chernyak and S. Mukamel, Localized electronic excitations in phenylacetylene dendrimers, *J. Phys. Chem. B*, 1998, **102**, 3310–3315 [Links].

17 R. J. Magyar, S. Tretiak, Y. Gao, H.-L. Wang and A. P. Shreve, A joint theoretical and experimental study of phenylene–acetylene molecular wires, *Chem. Phys. Lett.*, 2005, **401**, 149–156 [Links].

18 J. M. Seminario, A. G. Zacarias and P. A. Derosa, Theoretical analysis of complementary molecular memory devices, *J. Phys. Chem. A*, 2001, **105**, 791–795 [Links].

19 L. Jones, J. S. Schumm and J. M. Tour, Rapid solution and solid phase syntheses of oligo (1,4-phenylene ethynylene)s with thioester termini: molecular scale wires with alligator clips. Derivation of iterative reaction efficiencies on a polymer support, *J. Org. Chem.*, 1997, **62**, 1388–1410 [Links].

20 S. Rucareanu, O. Mongin, A. Schuwey, N. Hoyler, A. Gossauer, W. Amrein and H. U. Hediger, Supramolecular assemblies between macrocyclic porphyrin hexamers and star-shaped porphyrin arrays, *J. Org. Chem.*, 2001, **66**, 4973–4988 [Links].

21 N. Gonzalez-Rojano, E. Arias-Martin, D. Navarro-Rodriguez and S. Weidner, Bi-directional synthesis of a series of 2,5-dodecanoxy-phenyleneethynylene oligomers, *Synlett*, 2005, **8**, 1259–1262.

22 Y. Morisaki and Y. Chujo, Synthesis and properties of a novel through-space conjugated polymer with [2.2]paracyclophane and ferrocene in the main chain, *Macromolecules*, 2003, **36**, 9319–9324 [Links].

23 A. Fürstenberg, M. D. Julliard, T. G. Deligeorgiev, N. I. Gadjev, A. A. Vassilev and E. Vauthey, Ultrafast excited-state dynamics of DNA fluorescent intercalators: new insight into the fluorescence enhancement mechanism, *J. Am. Chem. Soc.*, 2006, **128**, 7661–7669 [Links].

24 A. Morandeira, L. Engeli and E. Vauthey, Ultrafast charge recombination of photogenerated ion pairs to an electronic excited state, *J. Phys. Chem. A*, 2002, **106**, 4833–4837 [Links].

25 J. P. Perdew, Density-functional approximation for the correlation energy of the inhomogeneous electron gas, *Phys. Rev. B*, 1986, **33**, 8822–8824 [Links].

26 A. Schäfer, H. Horn and R. Ahlrichs, Fully optimized contracted Gaussian basis sets for atoms Li to K, *J. Chem. Phys.*, 1992, **97**, 2571–2577 [Links].

27 R. Bauernschmitt and R. Ahlrichs, Treatment of electronic excitations within the adiabatic approximation of time dependent density functional theory, *Chem. Phys. Lett.*, 1996, **256**, 454–464 [Links].

28 R. Ahlrichs, M. Bär and M. Häser, Electronic structure calculations on workstation computers: the program system turbomole, *Chem. Phys. Lett.*, 1989, **162**, 165–169 [Links].

29 M. Häser and R. Ahlrichs, Improvements on the direct SCF method, *J. Comput. Chem.*, 1989, **10**, 104–111 [Links].

30 I. B. Berlman, *Handbook of fluorescence spectra of aromatic molecules*, Academic Press, New York, 1971.

31 A. Beeby, K. Findlay, P. J. Low and T. B. Marder, A re-evaluation of the photophysical properties of 1,4-bis(phenylethynyl)benzene: a model for poly(phenyleneethynylene), *J. Am. Chem. Soc.*, 2002, **124**, 8280–8284 [Links].

32 S. J. Strickler and R. A. Berg, Relationship between absorption intensity and fluorescence lifetime of molecules, *J. Chem. Phys.*, 1962, **37**, 814–822 [Links].

33 H. van Amerongen, L. Valkunas and R. van Grondelle, *Photosynthetic excitons*, World Scientific, Singapore, 2000.

34 A. Siemiarczuk, B. D. Wagner and W. R. Ware, Comparison of the maximum entropy and exponential series methods for the recovery of distributions of lifetimes from fluorescence lifetime data, *J. Phys. Chem.*, 1990, **94**, 1661–1666 [Links].

35 J. Wlodarczyk and B. Kierdaszuk, Interpretation of fluorescence decays using a power-like model, *Biophys. J.*, 2003, **85**, 589–598 [Links].

36 G. Verbeek, A. Vaes, M. Van der Auweraer, F. C. De Schryver, C. Geelen, D. Terrell and S. De Meutter, Gaussian distributions of the decay times of the singlet excited state of aromatic amines dispersed in polymer films, *Macromolecules*, 1993, **26**, 472–478 [Links].

Footnote

† This paper was published as part of the special issue in honour of David Phillips.